Environ. Sci. Technol. **1998**, *32,* 3318−3324

Formation of Pyromorphite in Anglesite-Hydroxyapatite Suspensions under Varying pH Conditions

PENGCHU ZHANG*
Sandia National Laboratories, Department of Geochemistry, MS 0750, Albuquerque, New Mexico 87185

JAMES A. RYAN
National Risk Management Research Laboratory, U.S. EPA, 5995 Center Hill Avenue, Cincinnati, Ohio 45224

Addition of phosphate to lead [Pb(II)]-contaminated soil to immobilize soil Pb by formation of pyromorphite has been proposed as an alternative remediation technique. Lead sulfate ($PbSO_4$, anglesite), a Pb-bearing form found in contaminated soils and wastes, was reacted with a synthetic phosphate mineral, hydroxyapatite [$Ca_5(PO_4)_3$-OH], under constant pH (pH 2−7) and simulated gastric pH conditions (pH varied from 2 to 7 within 30 min) to assess the effects of reaction kinetics on the formation rate of chloropyromorphite and the solubility of Pb. Under constant pH condition, complete transformation of anglesite to chloropyromorphite, [$Pb_5(PO_4)_3Cl$], was obtained at pH 4 and pH 5. At pH 6 and pH 7, the newly formed chloropyromorphite precipitated on the surface of undissolved apatite. The coverage of the apatite surface may reduce apatite dissolution rate and the transformation rate of Pb from anglesite to chloropyromorphite. Increasing the P/Pb ratio increased the transformation rate, but anglesite was still present after a 120-min reaction time. In the dynamic pH system, the added apatite was rapidly dissolved at the initial low pH, and complete transformation of anglesite to chloropyromorphite was obtained within 25 min. The soluble Pb level was controlled by the solubility of chloropyromorphite during the entire reaction process. These results demonstrate the effect of reaction kinetics on the formation rate of chloropyromorphite and the mechanisms controlling the solubilization of Pb in the anglesite−apatite system. Furthermore, they illustrate that a complete transformation of ingested anglesite to chloropyromorphite can be achieved under gastrointestinal tract pH conditions if sufficient phosphate is provided.

Introduction

Lead-contaminated soils are a major source of Pb exposure to children through ingestion, respiratory, and dermal uptake. The relationship between soil Pb and blood Pb concentrations in children has been demonstrated, and it has been illustrated that the soil Pb species, specifically the mineralogical forms, is a factor in determining the bioavailability of soil Pb (*1*−*3*). Therefore, in assessing the risk of exposure to Pb-contaminated soils, the geochemical forms of soil Pb should be considered. Furthermore, the concept of remediating Pb-contaminated soil by transforming the labile soil Pb species, i.e., soluble and bioavailable species, into the Pb chemical form that is stable under the environmental and physiological conditions of exposure is desirable.

Current technologies for contaminated soil remediation are usually costly (*4*) and/or cannot permanently prohibit the toxic element from entering into the biosphere. Thus, as an alternative remediation technique, in-situ immobilization of Pb in contaminated soils with phosphate amendments has received a great deal of attention in the past several years (*4*−*11*). This approach is based on the formation of geochemically stable lead phosphate minerals from the reactions of labile soil Pb forms with the added soluble phosphate salt or solid phosphate minerals such as apatite. Among the lead phosphate minerals, chloropyromorphite [$Pb_5(PO_4)_3Cl$] is the least soluble (*12*).

As the aqueous metal ions are recognized as the most mobile and bioaccessible species (*13*), the solubility of a metal species is generally an indication of its mobility, reactivity, and bioavailability. Reduction in bioavailability of soil Pb is a key issue in assessing the feasibility of in-situ immobilization of soil Pb. Attenuation of Pb concentration in aqueous solutions and the solutions of Pb-contaminated soils in the presence of hydroxyapatite [$Ca_5(PO_4)_3OH$] has been reported and is generally attributed to the formation of pyromorphite, $Pb_5(PO_4)_3$(Cl, OH, F...), from the precipitation of soluble Pb and phosphate (*6, 9*). In addition to the confirmation of reaction products from aqueous solutions, recent reports (*5, 14*) have presented direct evidences of formation of pyromorphite in Pb-contaminated soils amended with hydroxyapatite in suspension or in soil incubated under environmental conditions.

However, solubility is a thermodynamic parameter and determines the soluble Pb level only when the system is at equilibrium. In a dynamic system, the soluble Pb concentration depends on the solid Pb form that has the highest dissolution rate but not necessarily the highest solubility. The in-vitro experiment conducted by Ruby and co-workers (*15*) to simulate chemical processes within the mammalian digestive tract found the dissolution rate of different Pb sources to be dependent upon Pb mineralogy, with slow rates of Pb dissolution resulting in decreased Pb bioavailability. Furthermore, in soil−apatite incubation experiments it was found that the rates of soil Pb fractions reacting with the added apatite varied (*14*), demonstrating the effect of composition of Pb-bearing solids on the transformation rate of soil Pb species, and ultimately, on the bioavailability and mobility of soil Pb in a dynamic system. Thus, the transformation rate of soil Pb will vary with the dominant Pb-bearing form(s) in the soil amended with phosphate, and therefore, the efficiency of transforming soil Pb into pyromorphite by addition of phosphate mineral will be dependent upon the dissolution rates of the solid Pb-bearing forms in the soil and the added phosphate mineral as well as the rates of precipitation of pyromorphite.

In addition to the reaction occurring in soils, it has been speculated that the formation of pyromorphite may occur in the gastrointestinal tract (GI tract) when the contaminated soil is ingested with phosphate, thus successful reduction in soil Pb bioavailability requires a rapid and complete conversion of the chemically and/or biologically reactive Pb forms into pyromorphite. The dissolution rates of Pb-bearing forms and the amended phosphate mineral determine the rates of soluble Pb and phosphate (PO_4) released into solution, and

---

* To whom correspondence should be addressed: telephone: (505)844-2669; fax: (505)844-7354; e-mail: pzhang@sandia.gov.

S0013-936X(98)00232-6 CCC: $15.00

thus the rate of formation of pyromorphite. As the pH in GI tract varies rapidly with time after ingestion of a material, it is important to understand the effect of pH on the dissolution of Pb and phosphate minerals in relation to the precipitation rate of pyromorphite.

Anglesite, a secondary Pb mineral mainly resulting from weathering of galena (PbS) in acidic environment (*16*), is commonly found in mine wastes and soils (*2*). The bioavailability of Pb in anglesite-contaminated soils has been speculated to be determined by kinetic constraints, e.g., the dissolution rate, which controls the Pb solubilization (*1, 2, 17, 18*). To evaluate the reduction in bioavailability of anglesite in the presence of phosphate, anglesite and a synthetic hydroxyapatite were reacted under pH conditions found in the gastrointestinal fluid (pH 2−7) to assess the dissolution rate of the two minerals, the formation rate of pyromorphite, and the mechanism(s) that control(s) the Pb solubility during the reaction.

Methods

pH of Interest. The pH range of 2−7 was selected to simulate the pH values in the GI tract that has been discussed elsewhere (*19*). Reactions were carried out under static pH condition (pH-constant) and in suspensions in which the pH was adjusted from 2 to 7 within 30 min (pH-dynamic). This pH-dynamic system simulated the pH reactions in the GI tract and allowed determination of the potential transformation of Pb from anglesite to pyromorphite if anglesite and apatite were ingested simultaneously. It should be pointed out that the selection of pH range and time scale used was based on human physiology, but the results obtained can be applied to other reaction systems such as soil solutions and waste treatments.

Dissolution of Hydroxyapatite and Anglesite. Dissolution of anglesite and apatite was conducted in a 1.1-L glass beaker that contained a glass pH electrode and a stirring paddle. The beaker was placed in a water bath with a constant temperature of 37 °C. An automatic titrator was used to adjust and maintain the suspension pH with 0.1 N NaOH and 0.1 N HNO_3 solutions. One liter (1.0 L) solution of 0.100 M $NaNO_3$ and 0.001 M NaCl was adjusted to a desired pH prior to mineral addition. After mineral addition, the suspension was maintained at a constant pH and sampled periodically for 2−3 h. The suspension samples were filtered with a 0.2-μm membrane and analyzed for PO_4, SO_4, Ca, and Pb concentrations on an inductively coupled plasma spectrophotometer.

The synthetic hydroxyapatite used in this experiment was obtained from Bio-Rad. It has a specific surface area of 67.3 $m^2\ g^{-1}$ by BET nitrogen absorption and a P/Ca molar ratio of 1.62, which is close to the ideal ratio of 1.67. One to three grams (1.00−3.00 g) of apatite was used for dissolution rate determination. The dissolution of apatite was determined by measuring the soluble Ca and PO_4 concentrations as a function of reaction time.

The reagent lead sulfate ($PbSO_4$, obtained from Fisher Scientific) was examined by X-ray diffraction (XRD) analysis. The XRD patterns indicates that the solid is pure anglesite. A specific surface area of 0.9 $m^2\ g^{-1}$ was obtained by BET nitrogen absorption. One gram (1.000 g) of anglesite was used for dissolution rate determination. Soluble Pb and SO_4 concentrations were measured as a function of time to determine the dissolution of anglesite.

Reaction between Apatite and Anglesite. Determination of the kinetics of the apatite−anglesite reaction was conducted in the same reactor used in dissolution study. The amount of anglesite used to react with apatite was 1.5×10^{-5} mol, which was three times the anglesite solubility. Samples were periodically taken during the 120-min reaction period.

In the pH-constant study, the pH was adjusted to 2, 3, 4, 5, 6, or 7 and held constant for the 120-min reaction period. The amount of hydroxyapatite used was based on the molar ratio of phosphate to lead (P/Pb), with ratios of 3/5, 6/5, and 9/5 being used. These corresponded to 1, 2, and 3 times the amount of phosphate needed to transform the added Pb from anglesite into pyromorphite based on the 3/5 P/Pb ratio of chloropyromorphite, $Pb_5(PO_4)_3Cl$. The sampled suspensions were filtered with a 0.2-μm membrane and analyzed for soluble Ca, PO_4, Pb, and SO_4 concentrations.

In the pH-dynamic study, anglesite was reacted with apatite at a P/Pb molar ratio of 4.5/5. The solution pH was adjusted in increments of one pH unit from 2 to 7 over a 30-min time interval and then maintained at a pH of 7 for an additional 30 min. The suspension was sampled twice at each pH of 2, 3, 4, 5, 6, and 7. One sample was taken 1 min after the desired pH was established, and the second sample was taken before the pH was adjusted to the next pH value. The sampled suspensions were filtered with a 0.2-μm membrane and analyzed for soluble Ca, PO_4, Pb, and SO_4 concentrations.

In addition to the analysis of solution constituents, the solids in the reactor were collected by passing the reacted suspension through a 0.45-μm membrane. The solids were examined by XRD and scanning electronic microscope coupled with X-ray energy dispersive spectroscopy (SEM/EDX) for identification of minerals and the surface morphology and elemental composition.

Analytical Procedures. The soluble Ca, PO_4, Pb, and SO_4 concentrations were determined with an inductively coupled plasma spectrophotometer (ICP, Trace 61E, Thermal Jarrell Ash). The detection limit for the four elements was 2 $\mu g\ L^{-1}$. The U.S. EPA Water Supply Performance Evaluation Study (WS033) solution was used as the calibration standard. Experimental blanks, standards, and spiked samples were used for analytical quality control. Solution and suspension pH was measured by a glass pH electrode that was connected to a Mettler titrator. With this setup, the variation of pH could be maintained within 0.01 pH unit.

The solid samples were examined with an X-ray diffractometer (Scintag, XDS 2000; Cu Kα radiation, a potential of 30 kV filament current of 20 mA) and step-scanning at 0.04° 2θ/s was employed to obtain the XRD patterns for the powder samples. A scanning electron microscope coupled with energy-dispersive X-ray spectroscope (SEM/EDX, JEOL, JSM 5300) was used to obtain the solid images and elemental composition for the solids coated with carbon or gold.

A computer code for geochemical modeling of aqueous system, EQ3/6 (version 7.0), was used to estimate the species distribution for Pb(II), SO_4, Ca, Cl, and PO_4 and the degree of saturation in the suspension (*24*).

Results

Dissolution Rate of Hydroxyapatite and Anglesite. Dissolution rate of apatite was determined by measuring the concentrations of soluble PO_4 and Ca concentrations vs reaction time (Figure 1). The dissolution rate increases with decreasing pH, and below pH 4, the dissolution was too rapid to be accurately determined under these experimental conditions. Furthermore, a constant pH could not be maintained because of the rapid consumption of H^+ during dissolution:

$$Ca_5(PO_4)_3OH(s) + 7H^+ \Rightarrow 5Ca^{2+} + 3H_2PO_4^{2-} + H_2O \quad (1)$$

At pH 4, 1.2 (±0.2) g of added apatite dissolved within 80 min, resulting in a solution of $1.2 \pm 0.2 \times 10^{-2}$ M Ca and $7.2 \pm 1.1 \times 10^{-3}$ M PO_4. Based on the dissolution reaction (eq 1), these concentrations gave an activity product of $10^{14\pm1.2}$, which is close to the published solubility product (K_{sp}) of

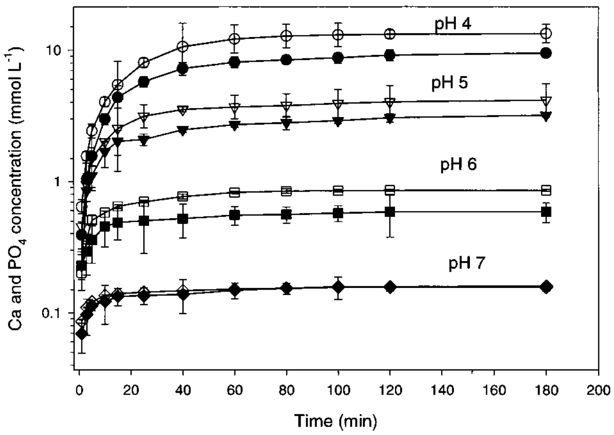

FIGURE 1. Dissolution of hydroxyapatite as a function of time and pH. The filled and unfilled symbols represent the phosphate and calcium concentrations, respectively. The error bars indicate the standard deviations of experimental replication.

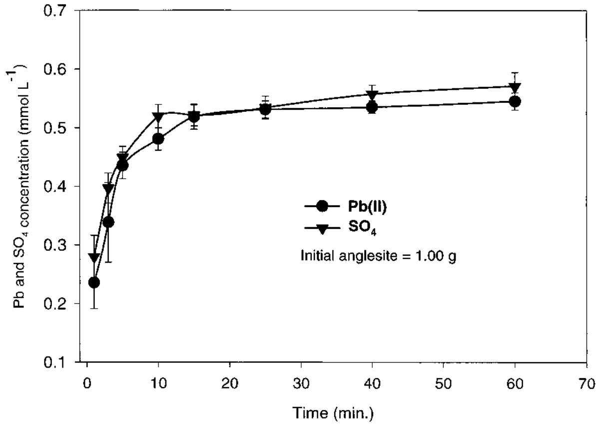

FIGURE 2. Dissolution of anglesite as a function of time. The data are averaged from anglesite dissolution occurring in the solutions with pH from 2 to 7. The error bars indicate the standard deviations of experimental replication.

$10^{15.8\pm1.7}$ (*20*). Thus, the solution was saturated with respect to apatite. At the relatively high pH values, e.g., pH 6 and pH 7, the dissolved Ca and PO_4 concentrations reached steady state in a shorter time period. This might be attributed to the effect of the total surface area of the solid apatite on dissolution rate. At pH 6 and pH 7, dissolution of apatite did not substantially reduced the added apatite surface area, only 1 and 4% of the total added mineral were dissolved at pH 7 and pH 6 within 60 min, respectively. In contrast, 20 and 40% of added apatite were dissolved at pH 5 and pH 4 within 25 min, respectively.

The soluble species compositions at pH 4, pH 5, and even pH 6 were stoichiometrically similar to that in apatite with a P/Ca molar ratio of 3/5 (Figure 1). However, at pH 7 the PO_4 and Ca concentrations were essentially the same. This can be attributed to Ca^{2+} adsorption on the undissolved apatite surface, which became negatively charged with increasing pH. Adsorption of Ca^{2+} reduced the soluble Ca concentration, causing the composition of soluble species to no longer be stoichiometric with respect to apatite.

In contrast to hydroxyapatite, dissolution of anglesite is independent of pH within the pH range of 2−7 (Figure 2). The dissolution of anglesite is a rapid process with saturation being reached within 20 min and about 45−55% of saturation concentration observed within the initial 3 min (Figure 2). Soluble Pb and SO_4 concentrations in the anglesite suspension vs reaction time indicated there was no significant effects of pH on dissolution in the pH range of 2−7 ($P = 0.05$) or on the stoichoimetric composition of the soluble species. Thus dissolution of anglesite follows the reaction:

$$PbSO_4(s) \Rightarrow Pb^{2+}(aq) + SO_4^{2-}(aq) \qquad (2)$$

At 60-min reaction, the activity product of Pb^{2+} and SO_4^{2-} was $10^{-7.3}$, which is very close to its reported solubility product, $K_{sp} = 10^{-7.8}$ (*21*). This implies little influence of adsorption or retention of dissolved ions by the anglesite, which has a low specific surface area of 0.9 $m^2\ g^{-1}$.

Reactions of Anglesite and Hydroxyapatite. It has been demonstrated that the dominant reaction in an aqueous system containing Pb^{2+} and soluble PO_4 is the formation of pyromorphite (*6, 11, 22, 23*). The product will be chloropyromorphite [$Pb_5(PO4)_3Cl$] if Cl^- is present in the aqueous phase. The results from previous experiments conducted in our laboratory have demonstrated that the formation of chloropyromorphite is a rapid process, completed within seconds. Therefore, the formation of chloropyromorphite is favorable in a PO_4-Pb-H_2O system, both thermodynamically and kinetically.

Considering chloropyromorphite formation from soluble Pb and PO_4 is instantaneous, the dissolution of hydroxyapatite and/or anglesite should be the rate-limiting factor in the overall reaction:

$$Ca_5(PO_4)_3OH(s) + 5PbSO_4(s) + Cl^- + H^+ \Rightarrow \\ Pb_5(PO_4)_3Cl(s) + 5Ca^{2+} + 5SO_4^{2-} + H_2O \quad (3)$$

Measurement of the concentrations of soluble species as a function of reaction time was the primary means of determining the reaction progress. The components dissolved from anglesite or apatite can be used to indicate the dissolution rates of the two minerals if they are not removed from solution during reaction. The distribution of species modeled from a geochemical computer code, EQ3 (24), indicated that the solutions were far from saturation for any possible calcium sulfate minerals. Thus, the total concentrations of Ca and SO_4 in solutions can be used to determine the dissolution of hydroxyapatite and anglesite, respectively. The differences between the dissolved and the measured PO_4 and Pb^{2+} were attributed to precipitation of chloropyromorphite.

pH-Constant Study. The concentrations of soluble Ca, SO_4, Pb, and PO_4 as a function of time were used to illustrate the dissolution rates of apatite and anglesite as well as the formation of chloropyromorphite. The concentrations of Ca and PO_4, 1.43 and 0.9 mmol L^{-1} at pH 2 after 10-min reaction, indicated complete dissolution of the added apatite (Figure 3a). The soluble Pb and SO_4 concentrations increased with time at nearly equivalent rates, implying that no dissolved Pb was removed from the solution. The concentrations of soluble Pb and SO_4 in the solution (Figure 3a) were approximately equivalent to that determined from suspension containing only anglesite (Figure 2). Apparently, the solution reached saturation with respect to anglesite but not chloropyromorphite. The results from the XRD analysis of the solids showed no detectable chloropyromorphite was formed after 120-min reaction, and the predominant mineral was the added anglesite (Figure 4a).

Complete dissolution of apatite was achieved within 10 min at pH 3 (Figure 3b). The soluble SO_4 and Pb concentrations were 1.0 and 0.1 mmol L^{-1}, respectively, indicating that 0.9 mmol of dissolved Pb was precipitated during the 10-min reaction time. The soluble PO_4 concentration was about 0.4 mmol L^{-1}, which suggested that about 0.5 mmol of PO_4 was removed from the solution. This amount of PO_4 was equivalent to that needed to precipitate the 0.9 mmol of dissolved Pb as chloropyromorphite. The formation of

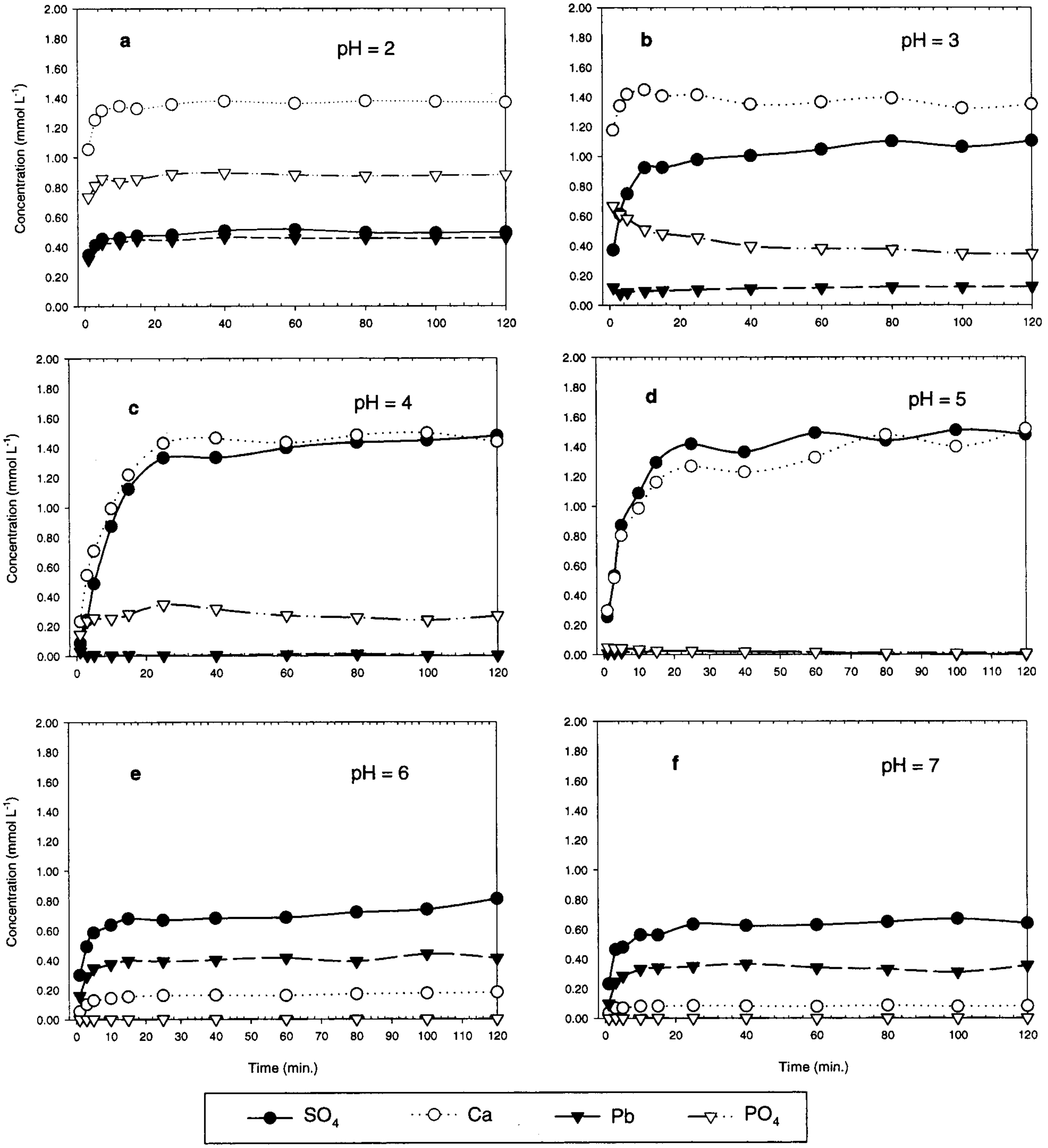

FIGURE 3. Concentrations of the soluble Pb, SO_4, Ca, and PO_4 in the anglesite−hydroxyapatite suspensions as a function of time. The P/Pb ratio in the suspensions was 3/5. Dissolution of anglesite and hydroxyapatite can be estimated from the soluble SO_4 and Ca concentrations, respectively.

chloropyromorphite was confirmed by the XRD patterns for the solid reacting at pH 3 (Figure 4b). The XRD patterns also indicated that anglesite was present and thus had not been fully transformed to chloropyromorphite.

Dissolution of apatite and anglesite at pH 4 (Figure 3c) was 100% and 95%, respectively, within 25 min. The soluble Pb was below 10^{-6} mol L^{-1} after 20 min, while the soluble PO_4 level was maintained at the level of 10^{-4} mol L^{-1} after 5 min. The XRD patterns of the solids indicate that both anglesite and chloropyromorphite are present but that there is nearly a complete transformation of anglesite-Pb into chloropyromorphite-Pb (Figure 4c). Similarly, at pH 5, approximately 95% of anglesite was dissolved within 20-min reaction (Figure 3d), and chloropyromorphite was the only mineral identified in the reacted solid after 120-min reaction (Figure 4d). Thus, complete transformation of Pb from anglesite to chloropyromorphite was achieved.

In contrast, the dissolution rates of hydroxyapatite at pH 6 and pH 7 were low, as demonstrated in Figure 3, panels e and f, respectively. The soluble PO_4 concentrations were insufficient to saturate the solution with respect to chloropyromorphite, even though the solution was rapidly saturated with respect to anglesite, whose dissolution rate was not pH dependent (Figure 2). This resulted in a very limited transformation of anglesite to chloropyromorphite during the 120-min reaction time. Furthermore, as the apatite surface became more negatively charged with increasing pH, Pb^{2+} was adsorbed from solution and chloropyromorphite

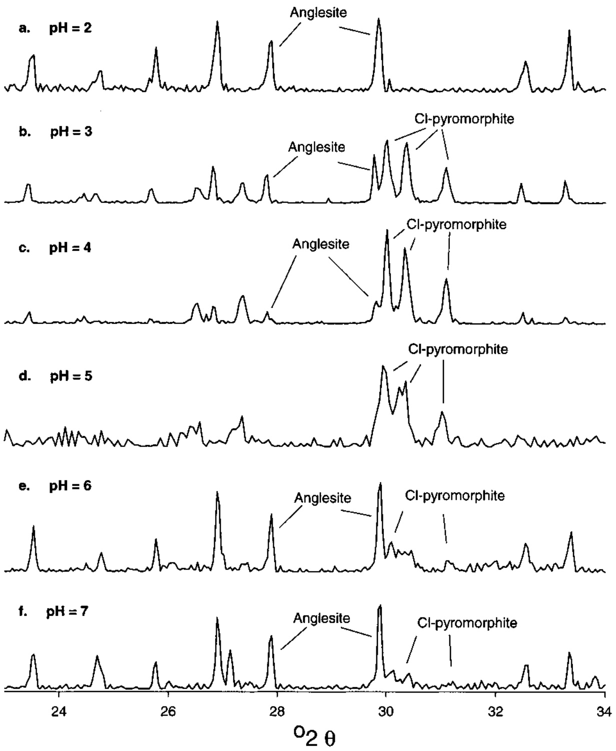

FIGURE 4. XRD patterns for solids collected from the anglesite−hydroxyapatite suspensions with pH after 120 min reaction, P/Pb = 3/5.

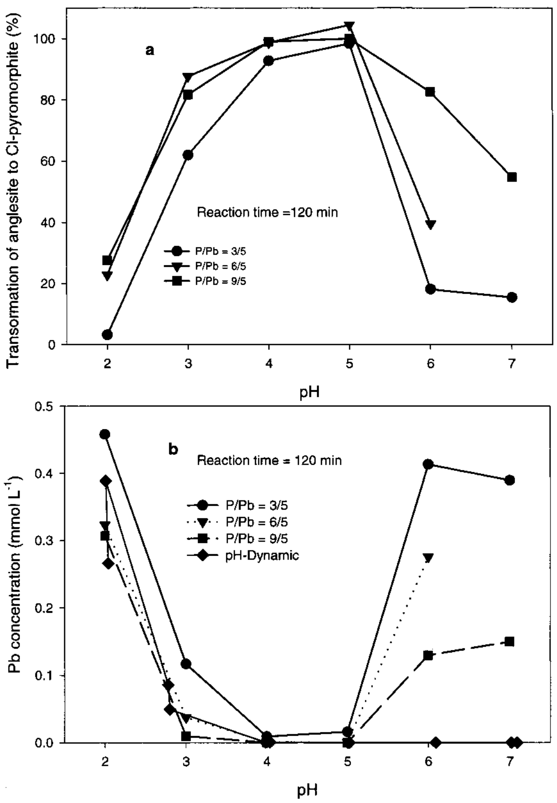

FIGURE 5. Effects of pH on dissolution of anglesite and transformation of Pb(II) from anglesite into chloropyromorphite in anglesite−hydroxyapatite suspensions (a) and on the soluble Pb(II) concentrations (b) after 120 min reaction for each of the three P/Pb ratios.

formed on the apatite surface (Figure 6b). The surface reaction may decrease or prevent apatite from further dissolution (*23*) and, therefore, reduces the formation rate of chloropyromorphite in the system. Consequently, the soluble Pb concentration at pH 6 and pH 7 was controlled by the solubility of anglesite (Figure 3, panels e and f). The XRD peaks for solids collected from anglesite−apatite suspensions at pH 6 and pH 7 confirmed limited formation of chloropyromorphite and that the added anglesite was the predominant mineral in the solid (Figure 4, panels e and f).

Effect of P/Pb Ratios. Similar results were observed in the suspensions with P/Pb = 6/5 and 9/5, as described in detail for P/Pb = 3/5 (Figures 3 and 4). To illustrate the effects of P/Pb ratios on the transformation rate of anglesite to chloropyromorphite and soluble Pb level in the apatite−anglesite systems, the results obtained after 120-min reaction from these three P/Pb ratios are presented together in Figure 5. The transformation of anglesite to chloropyromorphite was incomplete at low (pH 2 and 3) and high (pH 6 and 7) pH values for these three P/Pb ratios. The increase in P/Pb ratio increased the conversion of anglesite to chloropyromorphite, implying that soluble PO_4 was the limiting reactant and that the dissolution of apatite was the rate-limiting factor. At the intermediate pH values (pH 4 and 5), there was essentially complete conversion of anglesite to chloropyromorphite for all P/Pb ratios (Figure 5).

Effect of Solid Surface. In addition to the direct effect of dissolution rates of anglesite and apatite on the transformation process, the influence of the mineral surface on the reaction was also observed. At low pH values, the dissolution of apatite was rapid, and complete dissolution was achieved within 10 min (Figure 3a,b). Chloropyromorphite was observed to form in the solution at pH 3 (Figure 6a). In contrast, the dissolution rate of apatite is slow at pH 6 and pH 7, and the undissolved hydroxyapatite provided a surface for Pb^{2+} adsorption from solution. Furthermore, the hydroxyapatite surface served as the host for nucleation of chloropyromorphite (*23, 25*). The fine needle-shaped chloropyromorphite (confirmed by EDX) coated the surface of apatite in the suspension at pH 6 after 120-min reaction (Figure 6b). This coating might further reduce the dissolution rate of hydroxyapatite and result in reduction in the transformation rate of Pb from anglesite to chloropyromorphite.

pH-Dynamic Study. For the reaction conducted with pH varying from 2 to 7, the added hydroxyapatite (0.22 g) was completely dissolved during the first 5 min, and a high soluble PO_4 concentration (1.3×10^{-3} M) was established at the initial low pH (Figure 7). The soluble PO_4 concentration then decreased with time and pH and stayed stable at 2−3 $\times 10^{-4}$ M after 20 min (Figure 7). Because of the availability of soluble PO_4, the dissolved Pb from anglesite was rapidly precipitated into chloropyromorphite and the soluble Pb concentration quickly decreased from 4×10^{-4} mol L^{-1} at pH 2 to 10^{-7} mol L^{-1} within 5 min, at pH 3. The soluble-Pb concentration remained at 10^{-8} M thereafter. Complete anglesite dissolution was achieved between 20 and 25 min, as indicated by the soluble SO_4 concentration (Figure 7). The lack of Pb and PO_4 in solution suggests a complete transformation of Pb from anglesite into chloropyromorphite during this time period. With increasing pH, the dissolved apatite might have reprecipitated from solution, causing a decrease in the soluble phosphate level. Slightly decreasing Ca concentration, ranging from 1.8 to 2.1×10^{-3} mol L^{-1}, with increasing pH and time implies limited precipitation of apatite from the dissolved Ca and PO_4 could occur when the suspension pH increased. However, the only mineral in the reacted solid identified by XRD analysis after 120 min was chloropyromorphite (not shown). Therefore, more than 90% of phosphate removed from solution was consumed by precipitation of Pb as chloropyromorphite.

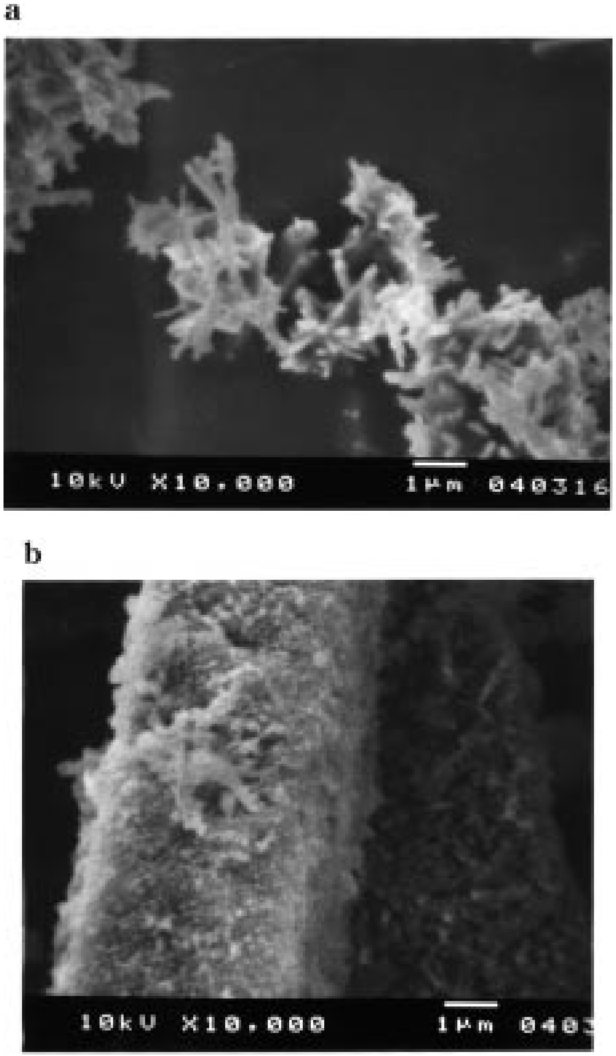

FIGURE 6. SEM images for the solids collected from the anglesite–hydroxyapatite suspensions at pH 3 (a) and pH 6 (b). The precipitate of chloropyromorphite occurred in solution at pH 3. At pH 6, the surface of undissolved apatite was covered by the precipitate, which may reduce the dissolution rate of apatite.

Discussion

The effects of solution pH on transformation of anglesite to chloropyromorphite and the soluble Pb level are attributed to the pH dependence of the solubility of chloropyromorphite and the dissolution rate of hydroxyapatite. At low pH values, the solubility of Pb from chloropyromorphite is comparable with that of anglesite. The solution might at first be saturated with respect to anglesite. For example, at pH 2, the soluble phosphate concentration from the added apatite at P/Pb of 3/5 is lower than 10^{-3} M, thus, the soluble Pb activity has to be $10^{-3.5}$ or higher in order to saturate the solution with respect to chloropyromorphite (*20*), while it is only $10^{-3.89}$ for anglesite (Figure 2). Thus, the solution is saturated with respect to anglesite, and the soluble Pb concentration is determined by the solubility of anglesite (Figure 5b). Accordingly, precipitation of chloropyromorphite under these conditions was limited. About 35% of added anglesite was dissolved at pH 2, and this was equal to that found in the suspension containing only anglesite, as shown in Figure 2. As the amount of apatite is increased to P/Pb ratios of 6/5 and 9/5, the soluble PO$_4$ concentration would be 1.8 and 2.7×10^{-3} M, respectively, assuming complete dissolution of the added apatite. These soluble PO$_4$ levels saturated the solutions with respect to chloropyromorphite and resulted in the precipitation of chloropyromorphite. The removal of dissolved Pb (Figure 5b) and the XRD analysis clearly demonstrated the presence of chloropyromorphite in the solids collected from the suspensions with P/Pb ratios of 6/5 and 9/5 at pH 2 after 120-min reaction (not shown). However, the removal of soluble PO$_4$ from solution resulted in the solution becoming undersaturated with respect to chloropyromorphite. Therefore, the precipitation process stopped when 25–30% of anglesite-Pb was converted into chloropyromorphite for P/Pb = 6/5 and 9/5 at pH 2 (Figure 5a). At pH 4 or pH 5, the solubility of chloropyromorphite was several orders of magnitude lower than that at pH 2 and pH 3. Thus, the precipitation of chloropyromorphite rapidly removed the dissolved Pb from the solution and enhanced anglesite dissolution, resulting in a complete dissolution of anglesite and transformation of Pb from anglesite to chloropyromorphite (Figure 5a), regardless of the P/Pb ratio. At pH 4 and pH 5, the dissolution rate of apatite was relatively high and provided adequate soluble phosphate for the precipitation of chloropyromorphite (Figures 1 and 3, panels c and d). The combination of the low solubility of chloropyromorphite [$-\log K_{sp} = 84.4$ (*26*)] and the high dissolution rate of apatite made it possible for complete anglesite dissolution and transformation to chloropyromorphite at these pH values. In the suspensions with pH 6 and pH 7, the dissolution rate of apatite was substantially decreased (see Figure 1) and the amount of dissolved PO$_4$ was limited. Thus, removal of dissolved Pb was slow, and the solution was saturated with respect to anglesite as the dissolution rate of anglesite is pH independent (Figure 2). Therefore, incomplete transformation of Pb from anglesite to chloropyromorphite was obtained (Figure 5a). As with the low pH system, in the high pH system increasing the amount of added apatite provided higher dissolved PO$_4$ for the reaction, resulting in a higher transformation rate. At pH 4–5, 95–100% of the anglesite was converted to chloropyromorphite, it dropped to 20–80% and 18–60% at pH 6 and 7, respectively, depending upon the P/Pb ratio. Thus, incomplete transformation of anglesite to chloropyromorphite was attributed to deficiency in soluble PO$_4$ at low pH and slow dissolution rate at high pH (Figure 5a).

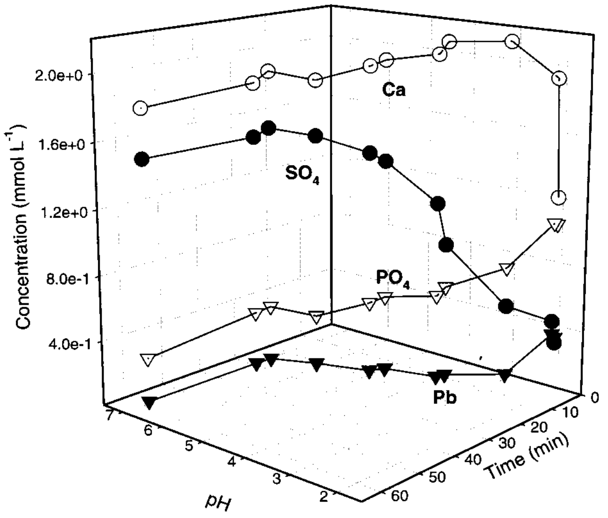

FIGURE 7. Effects of pH and reaction time on the concentrations of soluble species in the anglesite–hydroxyapatite system. The soluble SO$_4$ and Ca can be used to estimate the dissolution of anglesite and apatite, respectively. The difference between the soluble SO$_4$ and Pb is attributed to the precipitation of chloropyromorphite.

The transformation of Pb from anglesite to chloropyromorphite was incomplete, except at pH 4 and pH 5, within 120-min under the constant pH condition (Figure 5b).

However, in the pH dynamic system, a complete transformation was obtained within 25 min due to the rapid dissolution of apatite at initial low pH and precipitation of chloropyromorphite with increasing pH (Figure 7). Consequently, the soluble Pb concentration, an important index of bioavailability of ingested Pb, is determined by the solubility of chloropyromorphite [$-\log K_{sp} = 84.4$ (*26*)] at all pH levels in the pH dynamic system (Figures 5b and 7), whereas in a static pH system, it is determined by the solubility of anglesite at pH 2, pH 3, pH 6 and pH 7 (Figure 5b).

The primary concern of immobilization of soil Pb is reduction in bioavailability of soil Pb that may be ingested by a small child. The results from the pH-dynamic study illustrated that the transformation of biologically reactive Pb such as anglesite into chloropyromorphite can be completed within the time scale of the stomach emptying in the GI tract. The significance is that if the transformation of Pb from the labile soil Pb forms such as anglesite to chloropyromorphite is not completed prior to ingestion of the soil, the transformation is potentially completed in the GI tract and the bioavailability of soil Pb will be controlled by chloropyromorphite if there is stoichiometrically adequate amount of phosphate in the digestive system.

In a dynamic soil system, chemical properties including pH are subject to continuous change, as a result of seasonal changes in hydrology and temperature. Furthermore, changes in local environment such as between the rhizosphere and the bulk soil alter soil pH. These changes certainly affect the transformation rate of Pb from soil-Pb into lead phosphate minerals in phosphate-amended soil. Thus, prediction of the rate of transformation from experimental results conducted in a static fashion, i.e., fixed experimental conditions that have generally been adapted, will be in error.

Acknowledgments

The authors gratefully thank Drs. K. Brackett, P. Clark, and M. Schock for their assistance in SEM and XRD analysis. This research was supported in part by an appointment to the Postgraduate Research Participation Program at the National Risk Management Laboratory administrated by the Oak Ridge Institute for Science and Education through an interagency agreement between the U.S. Department of Energy and the U.S. Environmental Protection Agency. Although the research in this paper has been undertaken by the U.S. Environmental Protection Agency, it does not necessarily reflect the views of the Agency. Mention of trade names or commercial products does not constitute endorsement or recommendation for use.

Literature Cited

(1) Freeman, G. B.; Johnson, J. D.; Liao, S. C.; Feder, P. I.; Killinger, J. M.; Chaney, R. L.; Bergstrom, P. D. *Chem. Speciation Bioavailability* **1991**, *3*, 121−128.
(2) Ruby, M. V.; Davis, A.; Kempton, J. H.; Drxler, J. W.; Bergstrom, P. *Environ. Sci. Technol.* **1992**, *26*, 1242−1248.
(3) Davis, A.; Ruby, M. V.; Goad, P.; Eberle, S.; Chryssoulis, S. *Environ. Sci. Technol.* **1997**, *31*, 37−44.
(4) Berti, W. R.; Cunningham, S. D. *Environ. Sci. Technol.* **1997**, *31*, 1359−1364.
(5) Laperche, V.; Traina, S. J.; Gaddam, P.; Logan, T. J. *Environ. Sci. Technol.* **1996**, *30*, 3321−3326.
(6) Ma, Q. Y.; Traina, S. J.; Logan, T. J.; Ryan, J. A. *Environ. Sci. Technol.* **1993**, *27*, 1803−1810.
(7) Ma, Q. Y.; Traina, S. J.; Logan, T. J.; Ryan, J. A. *Environ. Sci. Technol.* **1994**, *28*, 408−418.
(8) Ma, Q. Y.; Traina, S. J.; Logan, T. J.; Ryan, J. A. *Environ. Sci. Technol.* **1994**, *28*, 1219−1228.
(9) Ma, Q. Y.; Logan, T. J.; Traina, S. J. *Environ. Sci. Technol.* **1995**, *29*, 1118- 1126.
(10) Ma, L. Q. *J. Environ. Qual.* **1996**, *25*, 1420−1429.
(11) Zhang, P.; Ryan, J. A.; Bryndzia, L. T. *Environ. Sci. Technol.* **1997**, *31*, 2673− 2678.
(12) Nriagu, J. O. *Inorg. Chem.* **1972**, *11*, 2499−2503.
(13) Logan, T. J.; Traina, S. J. In *Metals in Groundwater*; Allen, H. E., Perdue, E. M., Brown, D. S., Eds.; Lewis Publishers: Ann Arbor, MI, 1993; pp 309−347.
(14) Zhang, P.-C.; Ryan, J. A. Soil Science Society of America Annual Meeting, St. Louis, MO, 1995; ASA SSSA; 41.
(15) Ruby, M. V.; Schoof, R.; Eberle, S.; Sellstone, C. M. *Environ. Sci. Technol.* **1996**, *30*, 422−430.
(16) Blowes, D. W.; Reardou, E. J.; Jambor, J. L.; Cherry, J. A. *Geochim. Cosmochim. Acta* **1991**, *55*, 965.
(17) Jeffcoat, R. A. Research Triagle Institute for National Institute of Environmental Health Sciences: Research Triagle Park, NC, 1991.
(18) Hsieh, Y. H.; Huang, C. P. *J. Colloid Interface Sci.* **1989**, *131*, 537−549.
(19) Zhang, P.-C.; Ryan, J. A. *Environ. Sci. Technol.* In review.
(20) Nriagu, J. O.; Moore, P. B. *Phosphate Minerals*; Springer-Verlag: New York, 1983.
(21) Lindsay, W. L. *Chemical Equilibria in Soils*; Wiley & Sons: New York, 1979.
(22) Nriagu, J. O. *Geochim. Cosmochim. Acta* **1974**, *38*, 887−898.
(23) Xu, Y.; Schwartz, F. W. *J. Contam. Hydrol.* **1994**, *15*, 187−206.
(24) Wolery, T. J. Lawrence Livemore National Laboratory, Livemore, CA, 1992.
(25) Chen, X.; Wright, J. V.; Conca, J. L.; Peurrung, L. M. *Environ. Sci. Technol.* **1997**, *31*, 624−631.
(26) Dragun, J. *The Soil Chemistry of Hazardous Materials*; Hazardous Materials Control Research Institute: Silver Springs, MD, 1988.

Received for review March 10, 1998. Revised manuscript received July 6, 1998. Accepted July 27, 1998.

ES980232M